

Daily variations in stratification in İzmit Bay

Hüsne ALTIOK^{1*}, Lalehan CAN¹, Sabri MUTLU²

¹Institute of Marine Science and Management, İstanbul University, İstanbul, Turkey

²TÜBİTAK MAM Marmara Research Center, Environment and Cleaner Production Institute, Gebze, Kocaeli, Turkey

Received: 29.08.2019 • Accepted/Published Online: 07.04.2020 • Final Version: 01.07.2020

Abstract: We studied the diurnal variation of stratification in İzmit Bay with temperature and current velocity, and investigated the influence of atmospheric conditions. In the east of the bay entrance, 10-min temperature and hourly current measurements were made between the dates of 4 February 2015 and 24 April 2015, down to about 40 m depth in the water column. In addition to this, hourly temperature and salinity with depth data were collected between the dates of 4 and 7 February 2015 by a research vessel. The meteorological parameters for the atmospheric conditions were obtained from the closest weather stations (Yalova, Çınarcık, and Gebze). Thermocline depth varied between 20 and 30 m with instant changes at 6 to 35 m of depth due to strong wind conditions with 3 days of time delay. The south-westerly current directions were found in both layers, but the current speed decayed with depth. The high buoyancy frequency due to strong stratification decreased in strong wind and shear dominated the mixing process. Air pressure, air temperature, north-south component of wind and sea level had a semidiurnal cycle. A high-frequency measurement in a 2-layer system is highly significant to understand, explain, and determine the cause and effect relationships of hydrographic processes.

Key words: İzmit Bay, stratification, temperature-chain data, time series, diurnal changes, wind induced mixing, Richardson number

1. Introduction

İzmit Bay, ~50 km in length and 2–10 km in width, consists of 3 basins: eastern, central, and western basins (Figure 1). The eastern basin has a maximum depth of 30 m and connects with the central basin via a narrow strait. In the central basin, there are 2 deep regions (160 m and 200 m) close to the southern coast, which has a steep slope. The central and western basins are connected to each other by a narrow and short strait at a depth of about 50 m. The western basin is about 50-m-deep, deepens towards the Marmara Sea, and reaches a depth of 200 m. As a part of the Marmara Sea, İzmit Bay has a 2-layered water system. The highly saline lower layer water originated from the Mediterranean Sea (~38.5 psu) and enters the Marmara Sea through the Çanakkale Strait, sinks to the bottom, and reaches the İzmit Bay (Ünlüata et al., 1990; Beşiktepe et al., 1994). On the other hand, the less saline upper layer originated from the Black Sea (~18.0 psu) and flows through the İstanbul Strait into the Marmara Sea (Beşiktepe et al., 1994). Therefore, the İzmit Bay has a sharp-density interface with about 25 m depth as in the Marmara Sea (Ünlüata et al., 1990; Beşiktepe et al., 1994). The temperature and salinity of the upper layer water vary seasonally around 8.0 °C and 28.4 psu in winter and around 25 °C and 23.5 psu in summer. However, the

temperature and salinity of the lower layer display small seasonal variations. The mean temperature and salinity of the lower layer range between 13.4 °C and 36.9 psu in winter and 15.2 °C and 38.4 psu in summer (Algan et al., 1999).

The circulation patterns of the 2 layers change seasonally depending on the oceanographic characteristics of the Marmara Sea and the atmospheric conditions of the region (Sur, 1988). In spring and summer, the upper layer water flows into the bay due to sea level differences between the Marmara Sea and the interior of the bay. The upper layer flows towards the Marmara Sea in autumn and winter when the sea level differences are not effective. Strong winds, however, affect the circulation patterns and cause vertical mixing between the upper and lower layers at shallow depths (Baştürk et al., 1985; Sur, 1988; Algan et al., 1999; Altiook et al., 1996).

Since the İzmit Bay is one of the most industrialized and populated regions in Turkey, it has been subjected to many pollution studies. Types and amounts of pollution and chemical oceanographic characteristics, assimilation capacity, and nutrients that limit primary production were determined by Baştürk et al. (1985). Tuğrul et al. (1986) presented some results about water quality, wastewater loads, and their source in İzmit Bay. Okay et al. (2001)

* Correspondence: altiokh@istanbul.edu.tr

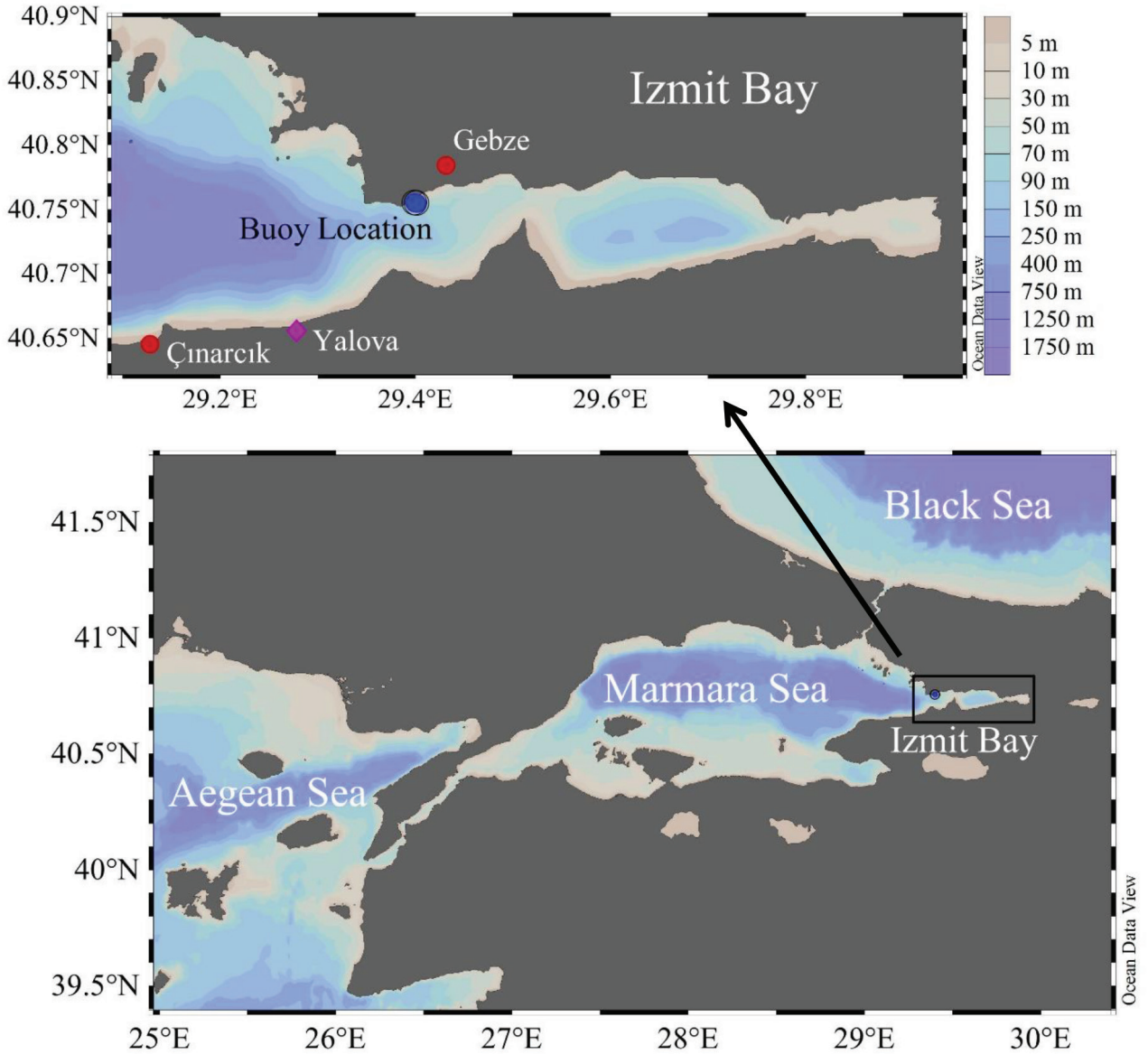


Figure 1. Location and bathymetry of İzmit Bay (the GEBCO_2014 grid, version 20150318, www.gebco.net).

and Karakoç et al. (2002) investigated pollution from the industry by measuring polycyclic aromatic hydrocarbons (PAH) and polychlorinated biphenyls (PCBs) in seawater, sediment, and mussels. The pollution effects of the 1999 earthquake in İzmit Bay were investigated by Balkis (2003) and Morkoç et al. (2007). An anoxic condition was observed due to great loads of industrial waste, which caused primary production in the upper layer, followed by lots of sink detritus to the bottom. Tolun et al. (2012) emphasised the importance of domestic wastewater treatment due to the decreasing water quality of İzmit Bay based on the integrated coastal zone management approach. They took into account the decrease of Secchi disc depth over the long term and more frequent harmful algal blooms,

as well as mucilage formations that occurred in İzmit Bay (Okay et al., 2001; Tüfekçi et al., 2010). Ergül et al. (2018) reported that there was a reproduction of phytoplankton by using nutrients coming from resuspensions of sediment after north-eastern storms.

The requirement of pollution monitoring in İzmit Bay is crucial as a pollution source into the Marmara Sea. The 2-layered stratification in the bay is influenced by hydrographic changes in the Marmara Sea. The mixing mechanism and material transport between the 2 layers vary daily, monthly, and annually based on the meteorological and oceanographic conditions in the Marmara Sea. The understanding of the mixing and exchange dynamics of the 2-layered system in the bay is

essential for rehabilitation studies on water quality. In this study, diurnal changes of stratification and the effects of atmospheric conditions in İzmit Bay were examined by using high-frequency data. The extensive dataset, including temperature chain (T-chain), Acoustic Doppler Current Profiler (ADCP) and conductivity, temperature and depth (CTD) measurements, and meteorological parameters allowed us to examine the frequency of stratification changes and response time between atmospheric and hydrographic variations of the 2-layered system in İzmit Bay. The measurements were made in the western basin of İzmit Bay where there are relatively low currents and low ship traffic (Figure 1). Although the dataset did not contain all seasons in a year, it was enough to analyse different wind regimes for investigation of the atmospheric influence on stratification since the measurement period was between the end of winter and the beginning of spring. The measurement period was between 4 February 2015 and 24 April 2015 for the T-chain and ADCP data. In the first 3 days of the measurement period, hourly CTD data were collected. CTD data allowed us to calculate some mixing parameters in the 2-layered system. The data are presented in section 2, results and discussion in section 3, and conclusions in section 4.

2. Materials and methods

Temperature and current velocity were measured by deploying a buoy located at a depth of ~50 m near the northern coast of İzmit Bay. This system consists of a buoy, moorings, and vault to set a T-chain and an ADCP at a fixed point. The measurements were obtained between 4 February 2015 and 24 April 2015 in the moored station. After deployment of the buoy system, hourly CTD measurements were made during the period of 4 February 2015 and 7 February 2015 in order to verify the T-chain data. During this period, CTD casts were made with SeaBird Instruments SBE25 Sealogger CTD, which was calibrated by the manufacturer, onboard the R/V Alemdar II.

T-chain: The T-chain was designed by mounting 24 temperature sensors (RBR, XR-420 model) on a cable at 1.5-m intervals. Each sensor had its own battery and memory card. The first sensor was placed at a 4.5 m depth for safety. The final sensor was at a depth of 39 m. Data acquisition was performed after removing the sensors from the water. Unfortunately, the data from the 20th sensor (at 33 m) were poor and had to be removed from the dataset. The time interval of the temperature measurements was 10 min. After the elimination of the bad data, hourly averaged temperature data were calculated for each depth.

Conductivity, Temperature, and Depth (CTD): The conductivity, temperature, and depth (CTD) data were measured by an SBE25 Sealogger during the period

between 4 and 7 February 2015. The accuracy rates of the sensors were 0.01 °C for temperature and 0.001 S/m for conductivity. The data quality of temperature and salinity was controlled manually after the cruise, and bad data in the profile were eliminated.

Acoustic Doppler Current Profiler (ADCP): The current velocity data were collected by using an RDI Workhorse Sentinel 300 kHz during the period between 4 February 2015 and 24 April 2015. The instrument, located at 4 m of depth, recorded current velocity data by the bottom track method. Both the bin size and the blank distance were set to be 2 m; therefore, the first reliable measurement was obtained from a depth of 8 m. To calculate the hourly current velocity profiles at the buoy deployment area, 60-s ensembles were carried out every 15 min.

Meteorological and sea level data: For the measurement period, hourly wind speed and direction, air pressure, and air temperature at Yalova, Gebze, and Çınarcık (Figure 1), and hourly sea level data at the Yalova station were obtained from the Turkish State Meteorological Service and Turkish National Sea Level Monitoring System (TUDES), respectively. The altitude of the meteorological station in Yalova is 4 m, whereas these altitudes were 130 m in Gebze and 16 m in Çınarcık. The wind speed was measured at 10 m high, while the air temperature was measured at 2 m. Air pressure was not reduced to the mean sea level. Sea level data were measured at a local datum and were not adjusted to any other reference station.

The linear equation approach was used in the trend analysis to calculate the diurnal changes of the air temperature, lower and upper layer sea temperatures in the 3 month period. The Welch method was used to estimate the spectral densities of the meteorological parameters, sea level, and sea surface temperature.

3. Results and discussion

3.1. Meteorological setting

Figure 2 displays the wind components (EW and NS) of Yalova, Çınarcık, and Gebze (see Figure 1 for locations of these stations) during the measurement period. The wind directions were almost the same at all stations, but the wind magnitude was higher at the Gebze station due to the station's altitude. Our deployment period between 4 February 2015 and 24 April 2015 covered several cyclonic passages that were dominant in the Marmara Sea (Alpar and Yüce, 1998). At least one strong northerly wind was observed each month. The strongest winds (up to 10 m/s) blew during the period of 9–13 February. In fact, the north-easterly winds were moderate (3–4 m/s). In February, the second north-easterly winds (maximum 8 m/s) were observed between 16 and 21 February, which was a long

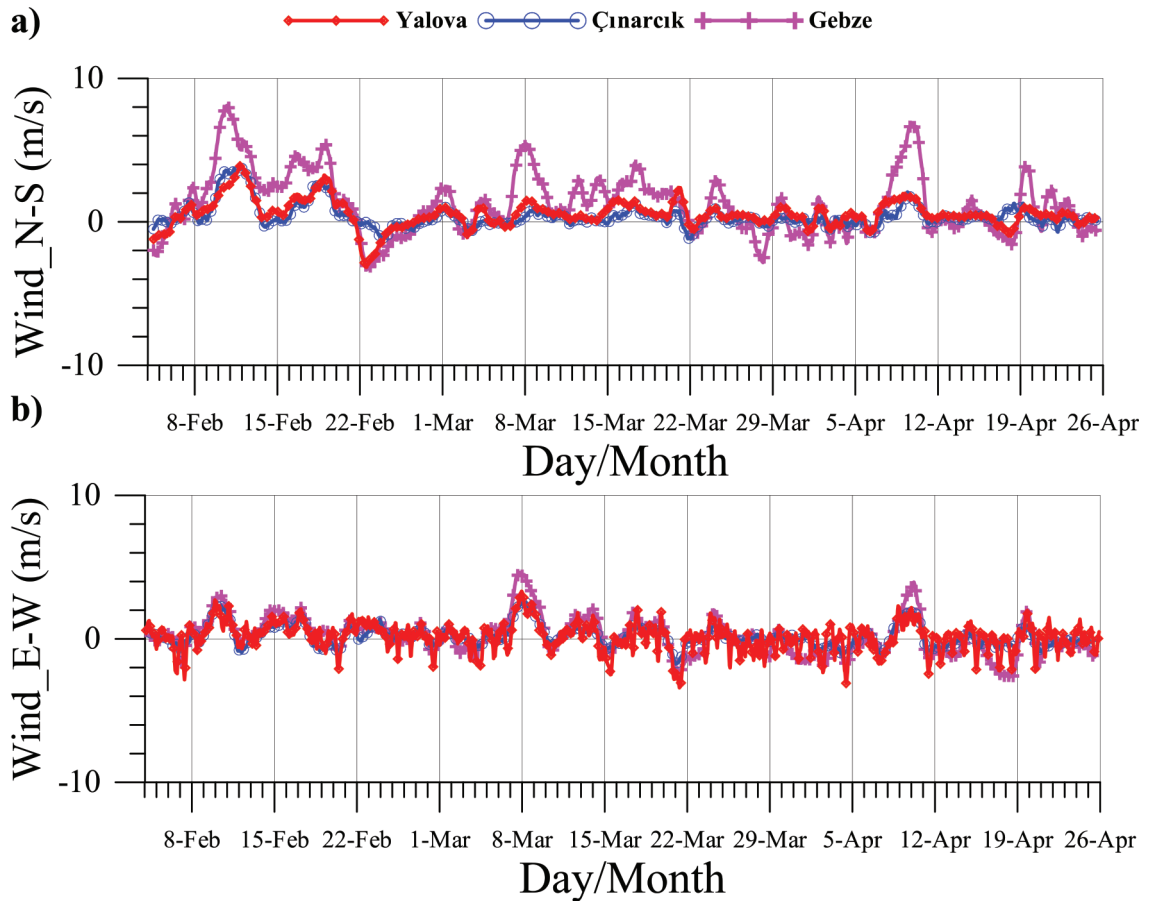


Figure 2. Moving average ($m = 23$) of hourly wind velocity at meteorological stations in Yalova, Çınarcık, and Gebze; a) north-south component; b) east-west component.

period with variable wind directions. The northerly wind periods were short and had less velocity in March and April (7–9 March and 9–11 April). The atmospheric pressure variations (Figure 3a) were compatible with air temperature (Figure 3b) and wind (Figures 2a and 2b), and they were high at low temperature. The temperature was low during the northerly wind period. On the first days of February, the air temperature was higher than the average temperature at all stations during the measurement period (8.5 °C). It was colder in the middle of February as northerly winds became dominant. At the end of February, the air temperature increased back again to above 8.5 °C. The monthly average air temperature was in the range of 5.7–7.3 °C in February, 7.9–8.9 °C in March, and 9.4–11.0 °C in April at all meteorological stations. The trends of air temperature over 3 months were 0.06 °C/day in Yalova, 0.07 °C/day in Çınarcık, and 0.08 °C/day in Gebze (Figure 3b), indicating that there could be atmospheric heating in the water column. The sea level height at the Yalova station (Figure 3c) reflected the variation in atmospheric pressure. The mean sea level was 20–30 cm lower during the northerly wind period.

3.2. ADCP observations

One of our main objectives was to examine the relationship between winds and stratification in İzmit Bay, which has a 2-layered system. The current velocity profiles obtained from the ADCP measurements during the period of 4 February–24 April were evaluated statistically and by a time series (Figures 4a–4d).

The time series of current magnitude (Figure 4a) displayed an evident increment in the current speed in some cases. The most evident feature was observed in February. The current speed (Figure 4a) was higher from the surface to deeper for several days. In this case, the strong northerly wind blew continuously for 5 days (9–13 February). At the end of this period, the maximum current speed was detected. This indicates that continuous windy days lead to a higher current speed in the bay. The other strong north-easterly wind periods (7–9 March and 9–11 April) were not as long (only 3 days). However, in March and April, the current speed was higher than average in these periods, too.

As seen from the time series of current velocity (Figure 4a), the current speed of surface water at up to

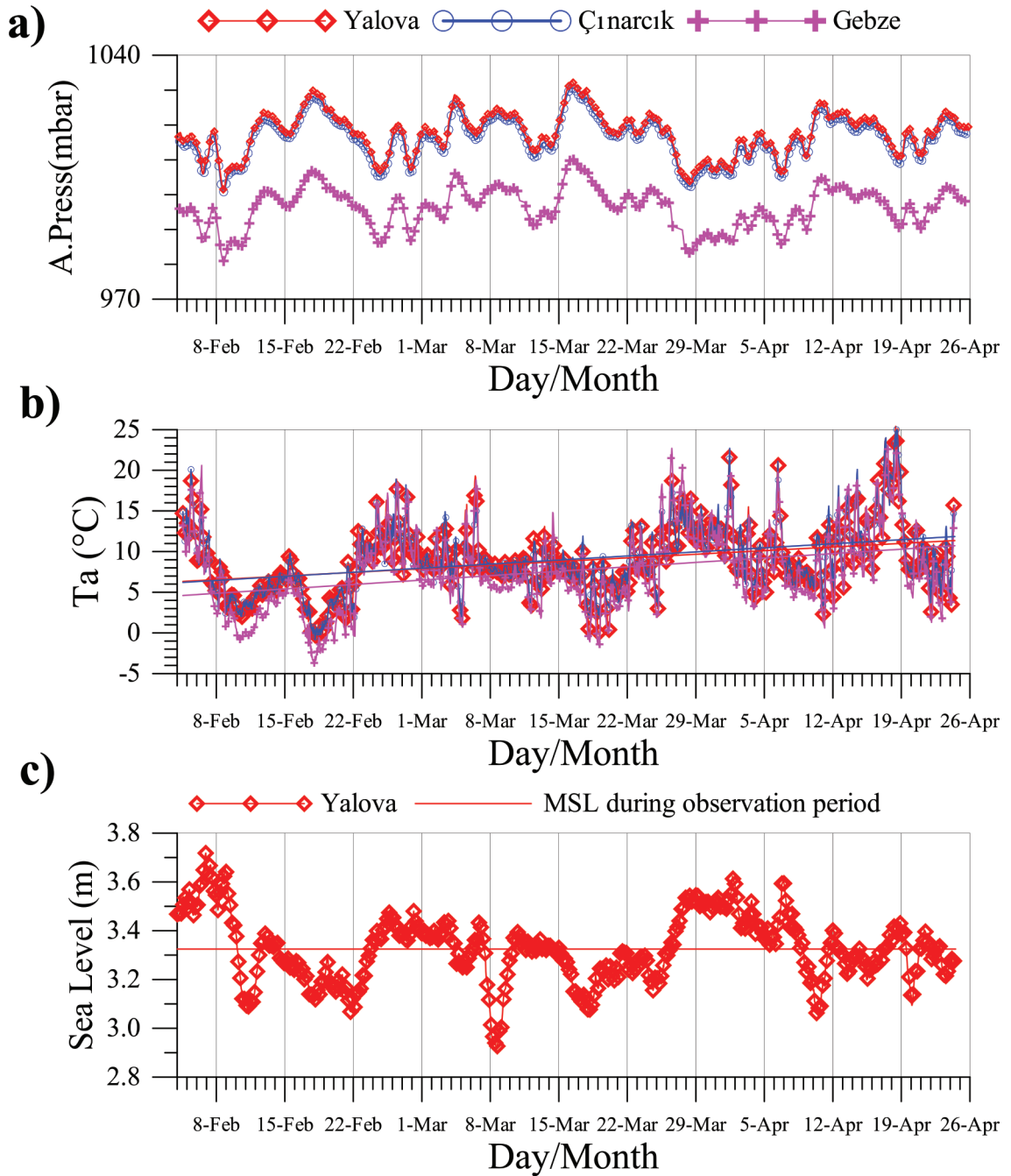


Figure 3. a) Air pressure (mbar); b) air temperature (°C) at meteorological stations in Yalova, Çınarcık, and Gebze, and c) sea level (m) at the Yalova station.

15 m depth was higher than those below. At the surface layer, the current magnitude was approximately 15 cm/s. On the other hand, the current magnitude at the lower layer was too small, and it decreased with depth. The current direction (Figure 4b) of the water column was the same for all layers and almost south-westerly during the measurement period. Statistically, for the upper layer

(10 m depth, Figure 4c), the most frequent direction and the highest current magnitude was south-westerly (220°–250°). South-westerly currents were almost 90% of the total at a depth of 10 m. In the lower layer at 34 m of depth (Figure 4d), the current magnitude decreased and the percentage of south-westward currents was almost 55%, whereas the other directions had very low current

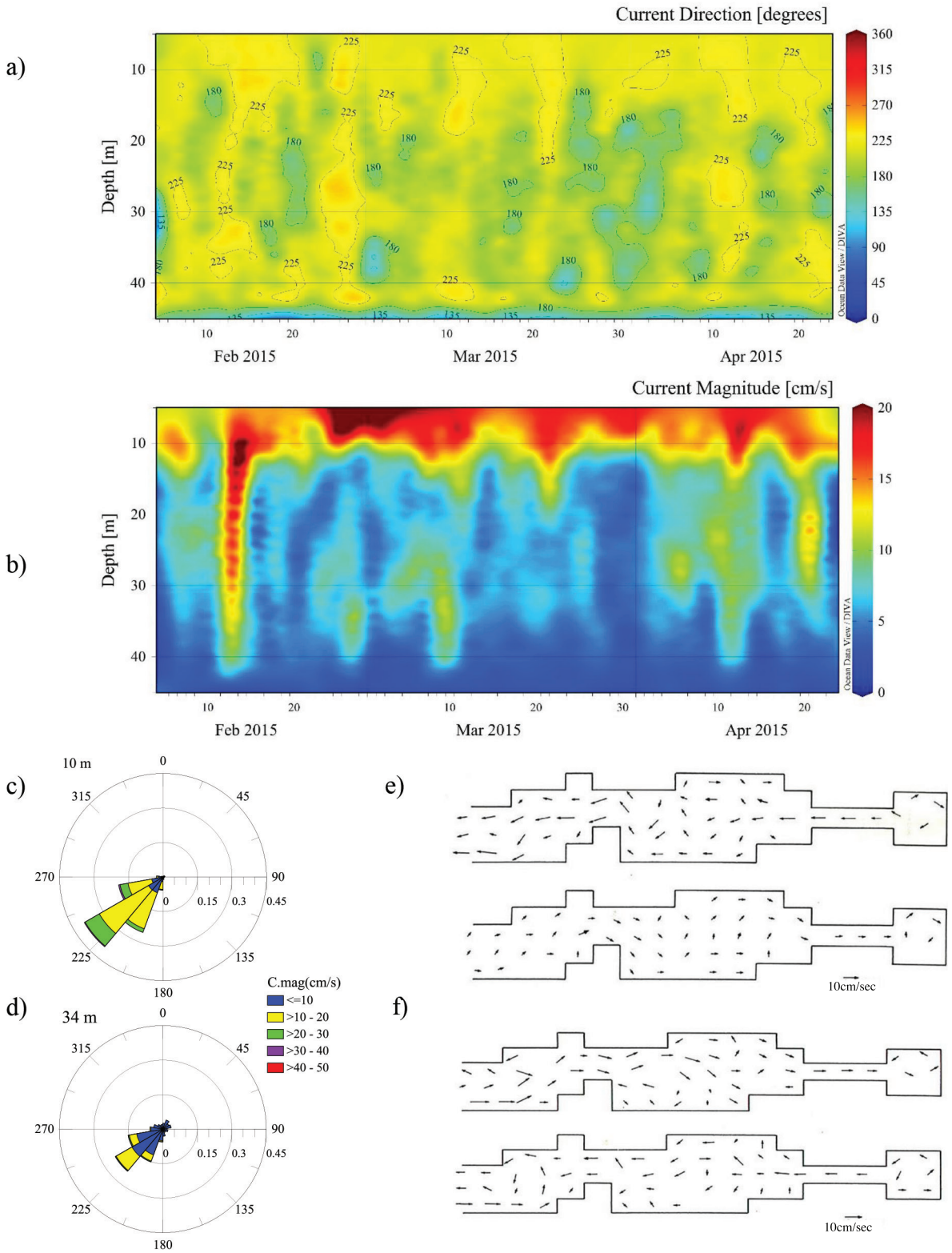


Figure 4. Current magnitude (cm/s) (a) and direction (degree) (b), time series, rose diagrams of the current velocity of depths of 10 m (c) and 34 m (d), summer (e) and winter (f) current circulation pattern of İzmit Bay (Sur, 1988) representing the upper and lower circulations in each graph, consecutively.

magnitudes. Higher current speed in the upper layer and lower current speed in the lower layer at the buoy location in İzmit Bay was close to the numerical model (Sur, 1988) where it was reported that wind plays a major role in surface circulation in İzmit Bay. The numerical model of Sur (1988) indicated that during the summer, the upper layer shows an inward current to İzmit Bay towards the shallow eastern basin, while the lower layer shows a pattern of water exit from the bay starting again from the eastern basin (Figure 4e). Conversely, in the winter season (Figure 4f), the circulation pattern of the lower and upper layers changes to indicate an inward flow of water towards the eastern basin in the lower layer and exits through the upper layer. Our observations indicated the same current direction at the location of the measurement buoy in both summer and winter circulation in accordance with Sur (1988), and higher current speed when the wind speed increased (Figures 4e and 4f). Although the current measurement at a fixed point did not provide any information about the circulation pattern in İzmit Bay, higher current speed indicated some justifications about the variation of the current pattern. In this situation, observations of higher current speed at higher wind speed supported Sur's (1988) model on the wind effects on the circulation pattern in İzmit Bay. The dramatic decrease in the sea level in Yalova generally led to a high current speed expectation in the bay and in our measurements. In this study, we investigated the effects of wind on variations of stratification, as well as the contribution of the changes of current speed and direction to stratification.

3.3. CTD observations

In order to investigate daily variations of stratification in the 2-layered system, we deployed T-chain and ADCP together. Unfortunately, the system did not include a conductivity sensor. To complete the information about density stratification, on the first 3 days, the CTD was deployed hourly. During the period between 4 February 2015 and 7 February 2015, temperature, salinity, and current data were obtained in calm weather conditions (Figure 2). The properties of both the upper and lower layers were typical winter conditions as given in the previous measurements. The temperature and salinity profiles during this period indicated the variation of interface depth in a range of 10 m (Figure 5). The surface temperature varied in the range of 9.7–10.6 °C with an average of 10.0 °C, and the lower layer temperature varied between 15.4 and 15.8 °C with an average of 15.5 °C. The variation in salinity was also low during this period. The mean salinity was 26.0 psu on the surface within the range of 25.6–26.4 psu, and the mean lower layer salinity was 38.6 psu within the range of 38.4–38.7 psu. The upper layer thickness fluctuated between 15 and 28 m, whereas the beginning depth of the lower layer fluctuated between 25 and 31 m. The interface temperature and salinity were in the ranges of 13.0–14.5 °C and 31.0–35.5 psu, respectively.

The temperature, salinity, and sigma-t time series for the period of 4–7 February 2015 are given in Figure 6. The cold and less saline upper layer is above the warm and more saline lower layer. Thermocline and halocline changes were in parallel to each other, and both caused a sharp

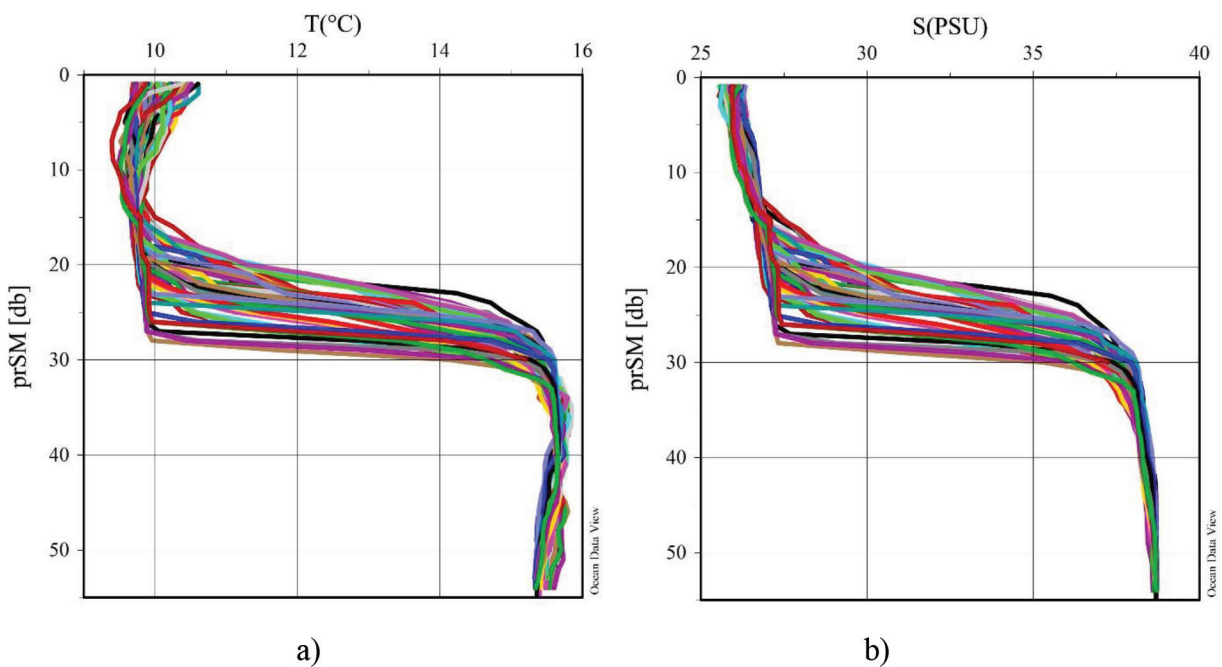


Figure 5. a) Temperature (°C) and b) salinity (PSU) profiles during the period of 4–7 February 2015.

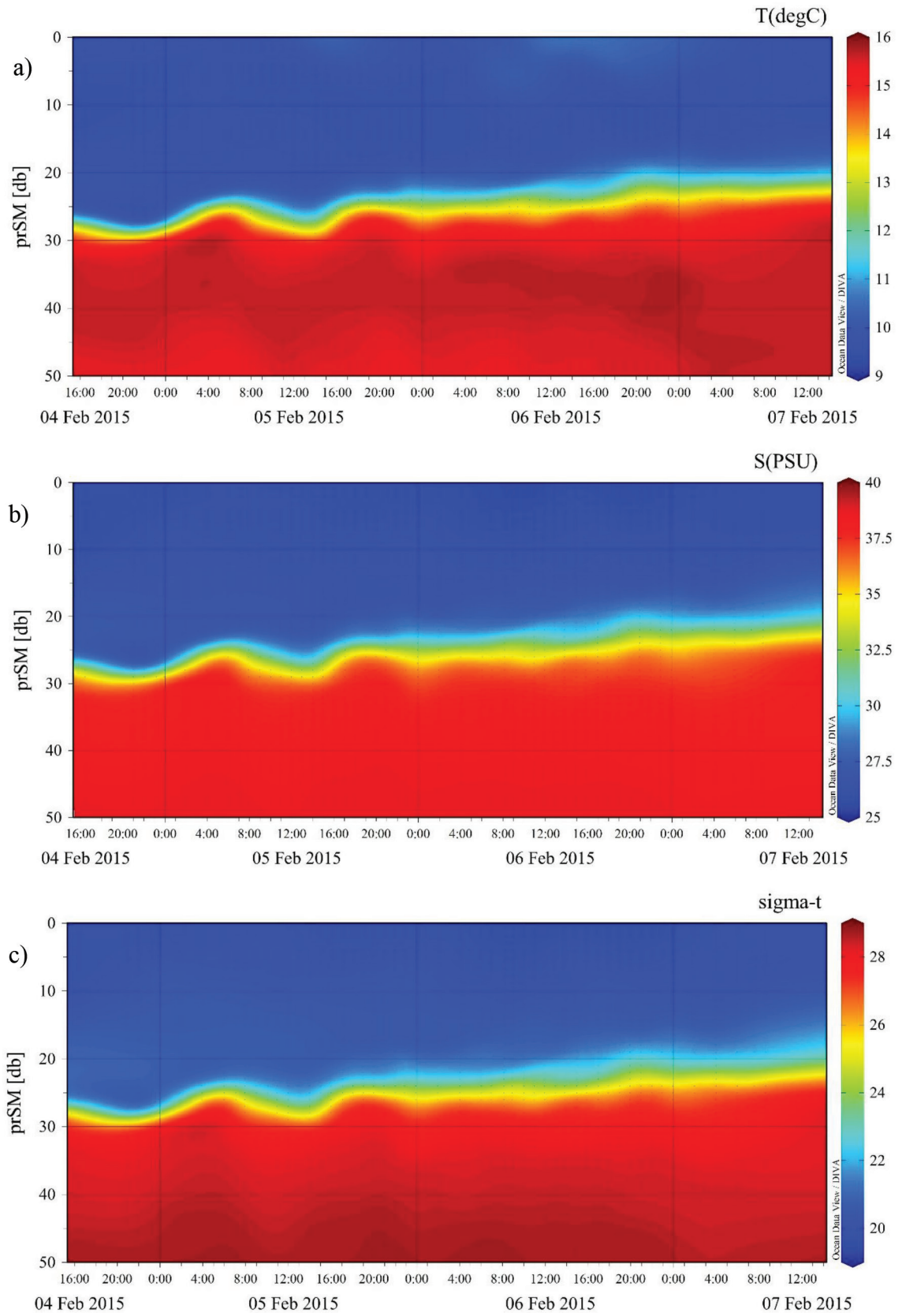


Figure 6. a) Temperature (°C), b) salinity (PSU), and c) sigma-t time series of the period of 4–7 February 2015.

pycnocline. As seen from the temperature and salinity profiles, there were only small changes in the temperature and salinity of the layers. However, it is clearly shown that there was a fluctuation at the interface depth for the first 2 days. On the third day, the interface depth slowly tilted to an upper depth. The current velocity (Figure 4b) indicated a unidirectional flow during the period of 4–7 February 2015. Surface water up to 15 m of depth had more than 10 cm/s velocity. The current magnitude of the upper and interface layer increased at mid-day on the third day, while the current direction veered between 220 and 250 degrees.

3.4. Mixing and advection parameters

Simultaneous measurements of CTD and ADCP allow a calculation of the Richardson number for the measurement period based on temperature, salinity, and velocity measurements. The vertical mixing parameter, the Richardson number, consists of both buoyancy and shear. The buoyancy (or Brunt Vaisala frequency) is the calculated density stratification ($N^2 = g/\rho \delta\rho/\delta z$), where g is gravity, ρ is density, and z is depth. The shear is calculated from the rate of velocity change by depth ($S^2 = [\delta u/\delta z]^2 + [\delta v/\delta z]^2$), where u and v are the horizontal velocity components. The Richardson number is the ratio of buoyancy to shear ($R_i = N^2/S^2$). When R_i is > 0.25 , the vertical structure is stable, whereas, when $R_i < 0.25$, the vertical shear will overcome the stratification and produce mixing (Turner, 1973).

The calculated shear and buoyancy frequency are given in Figure 7, where buoyancy frequency changed between $2 \cdot 10^{-5}$ and 0.03 s^{-2} , and shear changed between $0.03 \cdot 10^{-5}$ and 0.005 s^{-2} . It was noted that the buoyancy frequency was 10 times greater than the shear at higher values. On the other hand, the minimum value of shear was 100 times smaller

than the buoyancy frequency, where the stratification was very strong, and buoyancy frequency was very high, which means mixing was very difficult. If the current velocity has large changes with depth, shear is higher. It was expected that there would be no mixing in the interface due to the high Richardson number (Figure 8) since there was a large density difference ($\delta\rho/\delta z$). On the other hand, the current velocity gradient ($\delta u/\delta z$) caused a reduction in the Richardson number in the upper and lower layers, especially in the homogenous water column. Depths and time with small Richardson numbers (< 0.25) are indicated with density distribution in Figure 8. As it may be seen in the figure, mixing occurred below and above the interface. These regions could be found at 15–20 m of depth where the current speed changed with depth. Mixing regions in the lower layer were observed at 30–40 m of depth. The mixing duration took place from a few hours up to 7–8 h. This mixture procedure was not enough to weaken the density stratification in calm weather conditions. On the other hand, upward movement of the interface on the third day of observation might be related to sea level rise in Yalova, since the hydrographic conditions in İzmit Bay were influenced by the Marmara Sea. Accordingly, the analysis described above showed that vertical mixing could only occur when there was a higher shear value during the weak stratification process in İzmit Bay.

3.5. T-chain observations

To understand the atmospheric effects on the water column, temperature profiles are a suitable indicator, especially in transition seasons. The measurement period from February to April corresponds to the transition from winter to spring when atmospheric heating occurs. At

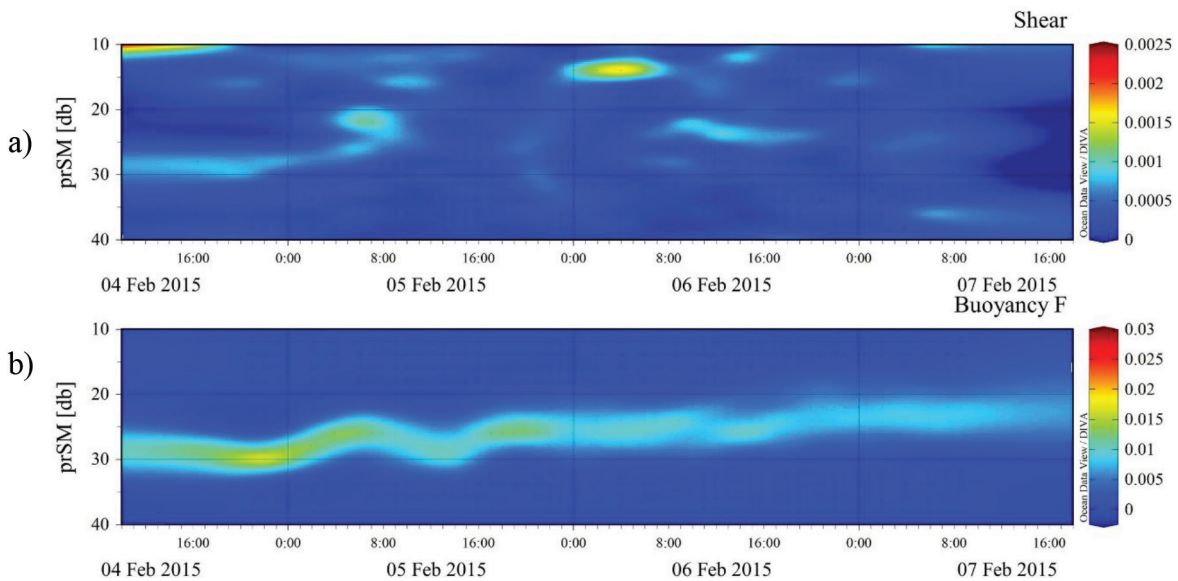


Figure 7. a) Shear (S^2 , unit: s^{-2}) and b) buoyancy frequency (N^2 , unit: s^{-2}) during the period of 4–7 February 2015.

the same time, the wind regime during this period allows us to catch stormy conditions. The other main objective was to investigate stratification variation according to wind speed. Unfortunately, the measurement period was cold according to the season average, which was 9.4 °C as the long-term average for February, March, and April (Turkish State Meteorological Service [https://mgm.gov.tr/]) and we could not observe atmospheric heating in the water column, but we could investigate the response of stratification to windy conditions. The hourly time series of temperature throughout the water column were

obtained by T-chain as given in Figure 9 for the period of 4 February – 24 April 2015. The temperature data showed a 2-layered structure during the observation period, although the interface variations occurred in a wide range. The thermocline depth was mainly observed between 20 and 30 m with extreme values of 6 and 35 m. The depth of thermocline may be assumed as an interface due to overlap with the pycnocline according to CTD observation. The upper layer temperature was 9.8 °C at the beginning of February. It decreased to 8 °C in the middle of February because of the cold air. It increased to 10 °C at the end of

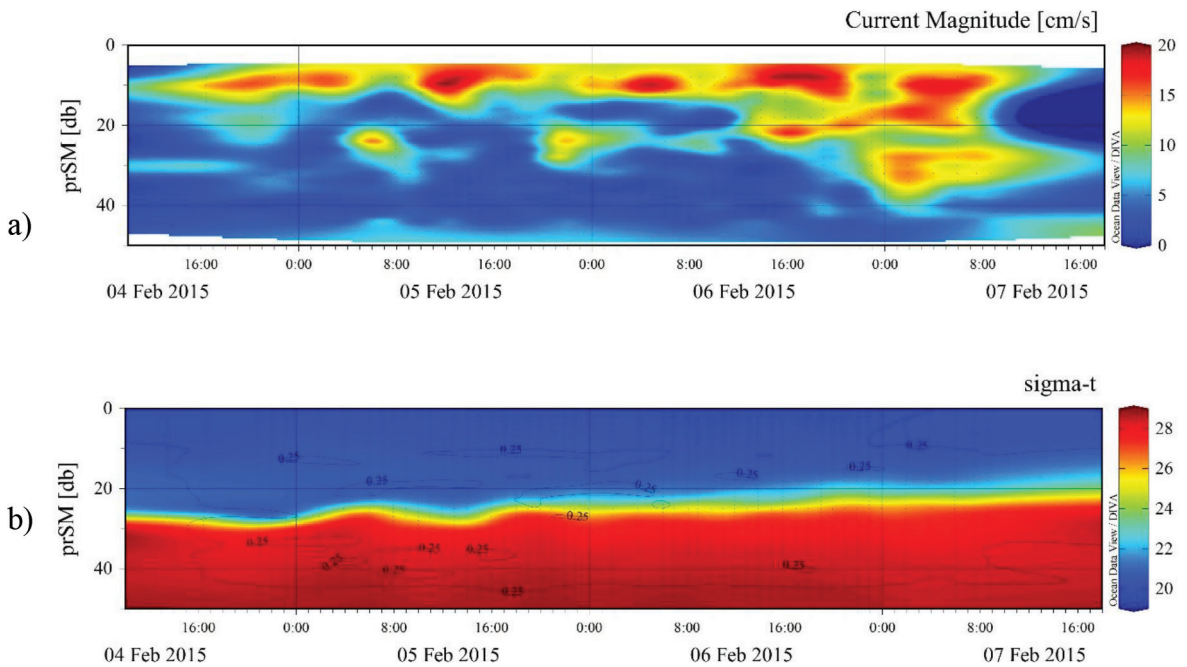


Figure 8. a) Current magnitude (cm/s), b) R_1 number (isolines, inside polygons $R_1 < 0.25$), and sigma-t (color scale) during the period of 4–7 February 2015.

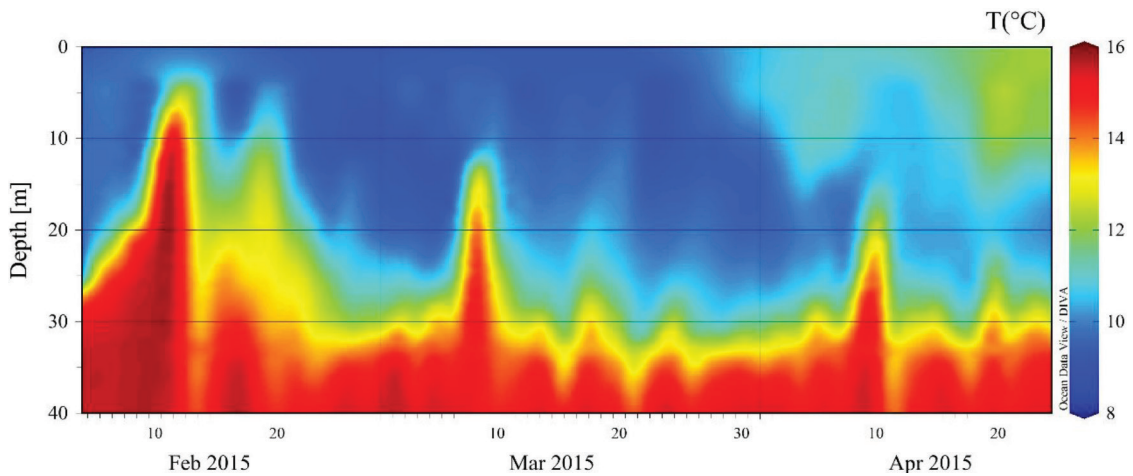


Figure 9. Time series of the temperature profiles measured by T-chain at buoy station during the measurement period.

March, while in April it reached 12 °C. The surface water (4.5 m) temperature changed between 8.8 °C and 13.8 °C, with an average of 10.2 °C and a standard deviation of 0.8 °C (Figure 10). In February, the surface temperature was in the range of 8.8–13.8 °C and its average value was 9.9 °C. In the second month of the observation period, in March, its average was 9.5 °C and its range was between 8.8 °C and 10.7 °C. In April, the surface temperature was in the range of 10.3–12.8 °C with an average of 11.3 °C. The air temperature was low during the period of 8–22 March (Figure 3a), the surface temperature decreased in March, and it was increasing again at the end of March, and in April.

On the other hand, the deep-water temperature (39 m) was in the range of 12.0–15.7 °C with an average of 15.2 °C and a standard deviation of 0.4 °C during the measurement period. Monthly variations of the deep-water were almost stable. In February, the temperature of the deep-water (39 m) was in the range of 13.3 to 15.7 °C with an average of 15.3 °C. In March, the deep-water was also colder (range: 12.0–15.7 °C, average: 15.1 °C). In April, the deep-water temperature was in the range of 12.6–15.6 °C with an average of 15.1 °C. The fluctuation of the temperature both at the surface and in the deep-water was related to mixing between the layers. The reason for the higher temperature of surface water in February was mixing between the upper and lower layers. In the lower layer, a temperature decrease with a short time delay was observed (Figure 10). As may be seen in Figure 9, a warm layer slowly occurred while the surface water temperature increased in accordance with atmospheric heating. At the same time, a cold layer above the thermocline could be seen.

It was obvious that the heating trend was higher in the surface water than in the deep-water during the 3 months.

The surface water had a 0.02 °C/day trend, and the bottom water had a -0.004 °C/day trend during the period of 4 February to 24 April. The minimum temperature of the surface water was observed in March unlike the minimum air temperature, which was observed in February.

3.6. Atmospheric influences on the interface

3.6.1. Wind effect on the temperature profile

During the measurement period, strong northerly winds lasting 3 days were recorded 3 times. The first strong north-easterly wind had continued for quite a long period between 9 and 13 February (5 days). Monitoring the temperature profile changes in these windy conditions help us see the wind effect on stratification. Figure 11a displays superimposed temperature profiles for each day at 12:00 (local time) before, during, and after strong north-easterly winds. In February, before the storm, the temperature profile indicated a very sharp interface, which was located between the depths of 18 and 21 m (number 1). One day later, the northerly wind started, and consequently, a more homogeneous and colder upper layer took place between the surface and a depth of 12 m. Meanwhile, the interface was getting thicker (12–24 m) (number 2), and the upper layer temperature was decreasing due to cold air coming with the wind. On the next day, strong winds dominated and the thermocline (number 3) moved up nearly 10 m higher (9–15 m). The day after the storm began, the thermocline was very sharp and placed between 5 and 8 m of depth (number 4). On the third day of the storm, the upper layer became absent (number 5). The temperature incline was up to 10 m of depth from the surface. During these 5 days, the lower layer's temperature was greater than 15 °C. One day later (number 6), the lower layer temperature and the surface temperature decreased below 14 °C and 12 °C, respectively. As given in Figure 4a, the

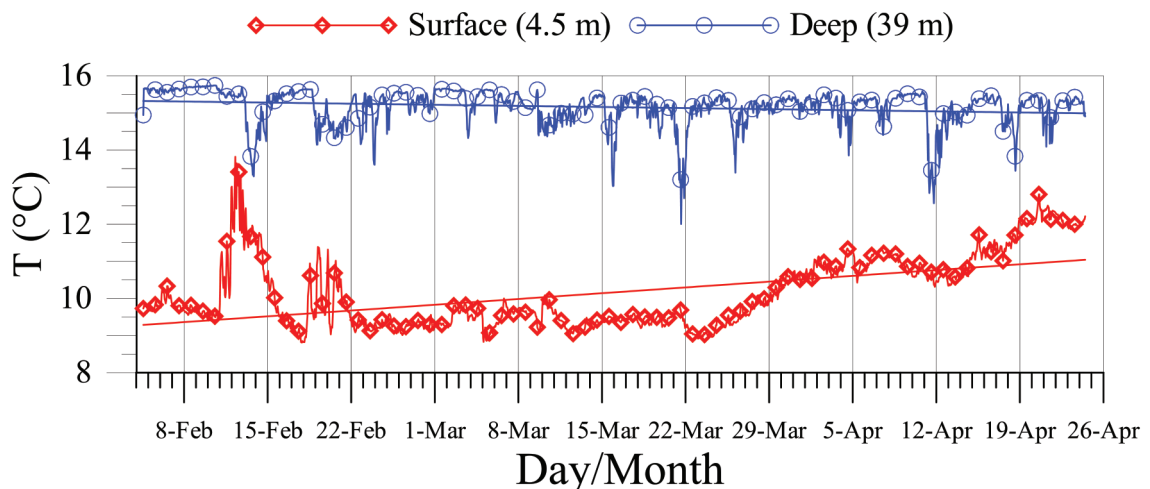


Figure 10. The temperature (°C) variations (line with symbol) and trends (line) of upper (4.5 m) and deep (39 m) water.

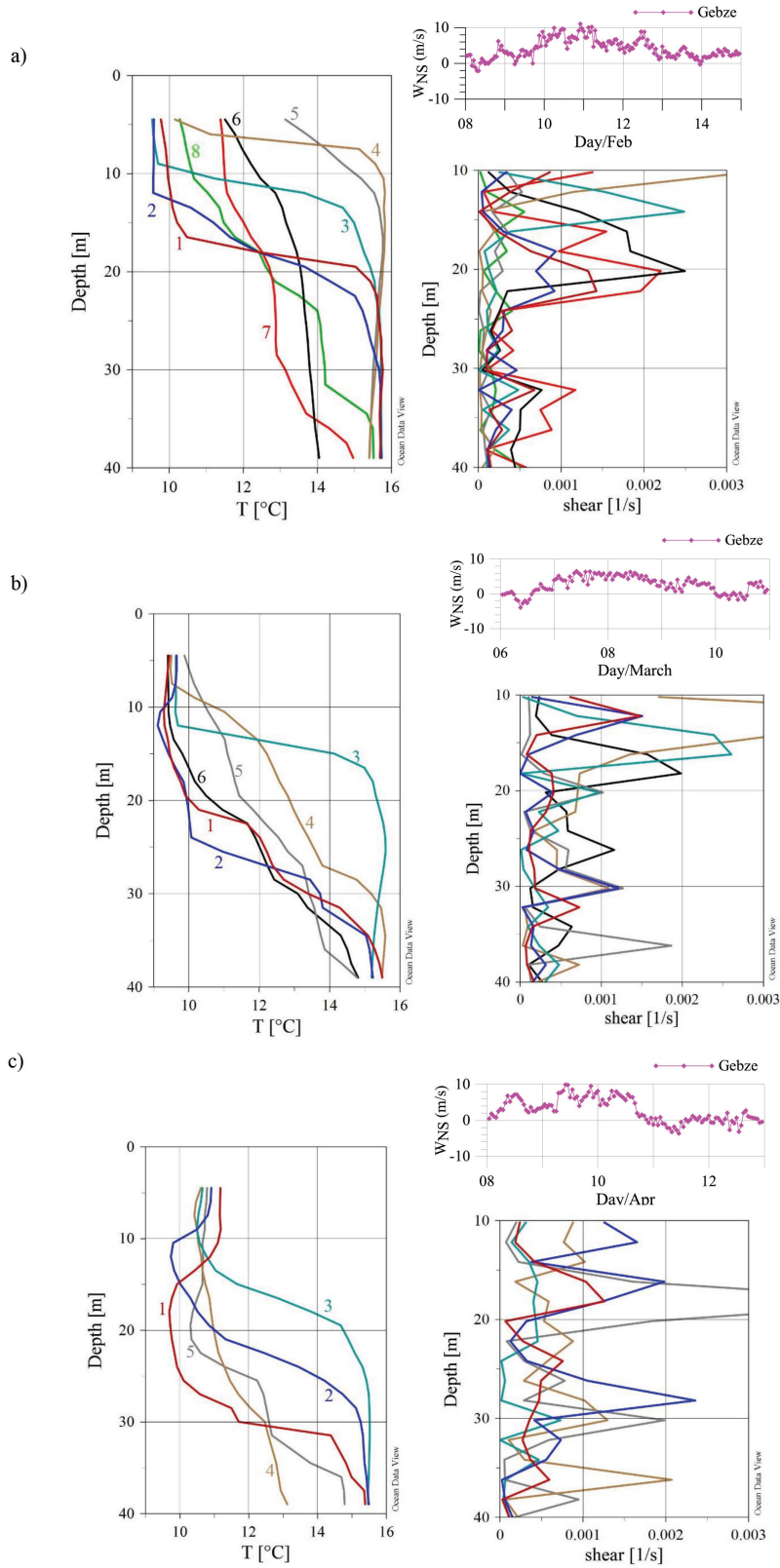


Figure 11. Temperature ($^{\circ}\text{C}$, left panel) and shear (s^{-1} , right panel lower part) profiles evaluation during stormy days (right panel upper part); a) numbers 1–8 refer to 8–15 February at 12:00 (local time); b) numbers 1–6 refer to 6–11 March at 12:00 (local time); c) numbers 1–5 refer to 8–12 April at 12:00 (local time).

magnitude of the current during this period increased throughout the water column, which indicated a lateral advection. This advection was a result of strong winds causing shallow water mixing in the eastern basin of the bay (Algan et al., 1999) and transport of this water mass due to circulation patterns (Sur, 1988) as given in Figures 4e and 4f. The calculated shear profiles are given together with temperature profiles (Figure 11b). The shear profiles of numbers 1–4 showed that the shear was maximal in the thermocline. These maximum values of shear did not cause any mixing since the calculated buoyancy frequency derived from density and current speed was too high in the pycnocline (Figure 7). Although salinity was unknown, temperature indicated a 2-layer stratification as well. On the other hand, the profile of number 6 indicated that all water column mixture had a maximum shear at a depth of 20 m. It may be stated that the mixing continued in this location. Strong northerly winds lasting 3 days forced the upper layer to pile in the southern coasts and the lower layer to rise due to continuity in İzmit Bay. In the northern coasts, the stratification almost disappeared, and the shear increased due to the higher current speed. After the storm, the 2-layered system reoccurred due to the absence of wind stress. The step structure of the temperature profiles indicated mixed layer generations during this process.

Although there was a shorter period of strong wind conditions, the other strong wind episodes given in Figures 11b and 11c showed similar characteristics.

If the northerly winds are dominant longer than 3 days, the depth of the upper layer decreases. At the same time, the interface depth rises to a higher depth, and then, the buoyancy frequency decreases in the weakly stratified water column. When the shear value is greater than the buoyancy frequency, until the Richardson number is less than 0.25, mixing occurs. The temperature profiles in these strong northerly wind conditions indicated clearly that the interface would be absent after 3 days of sustained

northerlies. The mixing leads to a warmer upper layer and a colder lower layer than these layers are under calm conditions.

3.6.2. Relationship with other atmospheric parameters

The interface depth varied between the surface and the bottom during the measurement period. As we explained in the sections above, the extreme values of interface depth resulted from wind effects. The interface depth could be defined as the depth of 14 °C temperature after examining the CTD measurements. Figure 12 displays the wind speed at the Gebze station and interface variations by time. This graph demonstrates not only the variations of interface depth due to wind forcing but also daily variations of other atmospheric effects. It contains the daily dramatic changes of the interface between the surface and the bottom under blustery conditions, as well as changes with various amplitudes. There was a strong correlation between the interface depth and wind speed with a time delay. The relationship between wind speed and the depth of the interface was investigated by calculating the Pearson's correlation coefficient by running the "corrcoef" function in MATLAB. The correlation coefficient r -value was -0.43 , and the P -value was less than 0.001, which means that there was a highly significant relationship between the variables. After investigation of the relationship between the variables, the response of the intermediate layer depth to the wind speed was also calculated by running the "finddelay" function. The result was 82. Since the data was hourly, it may be stated that the intermediate layer depth responded to the strong winds after 82 h (nearly 3.4 days). All 3 features indicated that after the interface depth was close to the surface, almost 3 days later, suddenly the interface depth disappeared because of the mixing of the water column.

To compare all meteorological parameters and upper layer temperature in daily variations, we conducted a

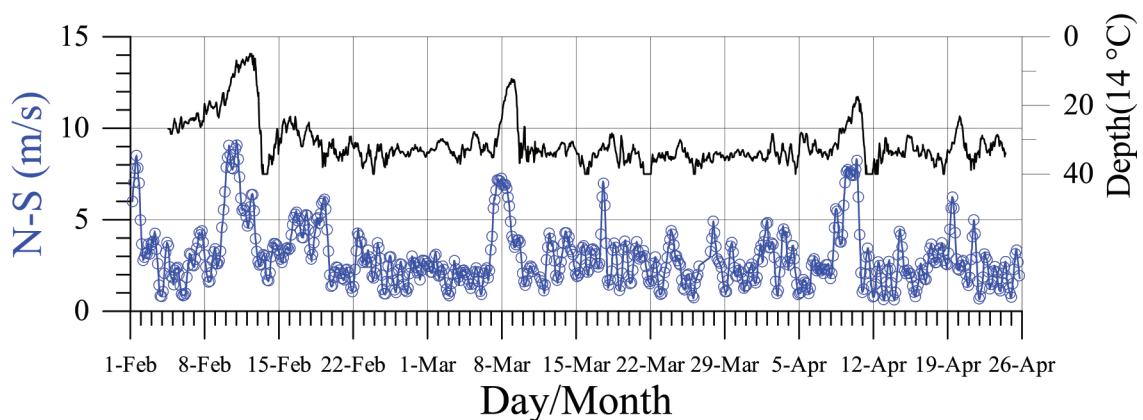


Figure 12. Wind speed (m/s) at the Gebze station and interface depth (m) of 14 °C temperature time series.

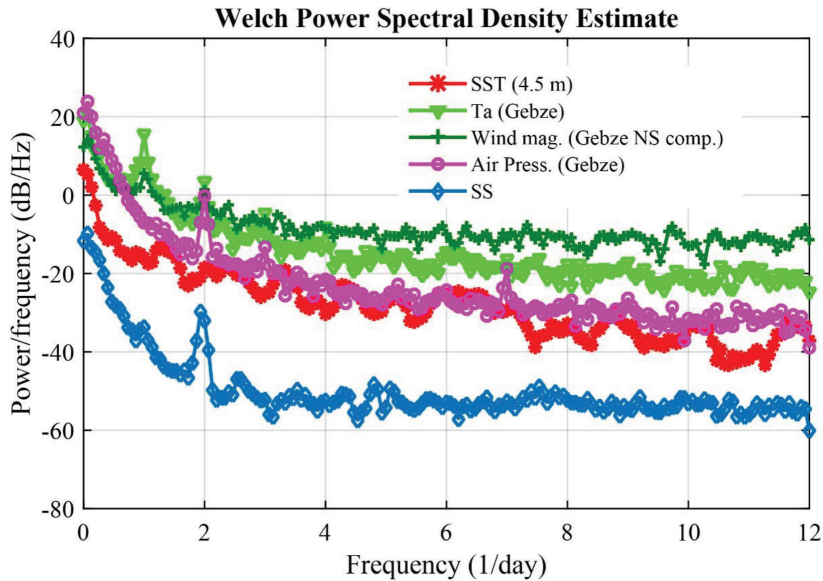


Figure 13. Spectral analysis of the parameters.

spectral analysis. Figure 13 displays the results of the spectral analysis of the meteorological parameters and sea surface temperature. Wind and air temperature had a diurnal cycle. Atmospheric pressure, air temperature, and the N–S component of wind, as well as the sea level in Yalova, had a semidiurnal cycle. However, there was no evidence that the upper layer temperature had any periodicity.

4. Conclusions

High-frequency observations in a 2-layered system showed that there is a highly complex dynamic structure in İzmit Bay. Hourly oceanographic and atmospheric data during the period of February to April were investigated in this study. This dataset provided us with an examination of the mixing process in a 2-layered system and the wind effects on stratification, as well as allowing us to conduct a time series analysis during the observation period, corresponding to the atmospheric heating period. The monthly average air temperature increased from 5.7 °C as the minimum to 11.0 °C as the maximum during the observation period because of dominant northerly winds. The air temperature trend was approximately 0.07 °C/day, while the sea surface temperature increased by 0.02 °C/day during this period with an average of 10.2 ± 0.8 °C. The average deep-water temperature of 15.2 ± 0.4 °C had a smaller standard deviation. The flows in both layers were in the same direction, which was south-easterly. However, the current speed of the upper layer was determined to be higher than that of the lower layer.

Continuous strong north-easterly wind conditions were observed 3 times (9–13 February, 7–9 March,

and 9–11 April 2015). The mean sea level decreased by 20–30 cm during the northerly wind period. The 2-layer stratification in İzmit Bay was affected by strong wind conditions. The thermocline depth obtained from T-chain data varied between the depths of 20 and 30 m with sudden fluctuations between 6 and 35 m in these periods.

Hourly CTD observation for 3 days provided us with the mixing characteristics of the 2-layered water column. The calculated Richardson number ($R_i = N^2/S^2$) showed the relationship between buoyancy frequency and shear. The wind caused a deterioration of stratification, and therefore, a smaller N^2 value was found. In these conditions, shear dominated the mixing, and it may be stated that shear was mainly responsible for mixing, while wind-induced the occurrence of mixing. The time delay between the beginning of the strong winds and the highest interface depth was calculated to be nearly 82 h (~3.4 days).

As expected from the spectral analysis, atmospheric pressure and air temperature, the NS component of wind, and sea level had a semidiurnal cycle. However, there was no evidence that the upper layer temperature had any periodicity due to lack of surface temperature information.

In conclusion, a high-frequency measurement in a 2-layer system contains significant information in order to understand, explain, and determine the cause and effect relationships of hydrographic processes.

Acknowledgment

This study was supported by the Scientific and Technological Research Council of Turkey (TÜBİTAK) under project 110Y244.

References

- Algan O, Altıok H, Yüce H (1999). Seasonal Variation of Suspended Particulate Matter in Two-layered İzmit Bay, Turkey. *Estuarine, Coastal and Shelf Science* 49: 235-250. doi: 10.1006/ecss.1999.0494
- Alpar B, Yüce H (1998). Sea-level variations and their interactions between the Black Sea and the Aegean Sea. *Estuarine Coastal and Shelf Science* 46: 609-619.
- Altıok H, Legovich T, Kurter A (1996). A Case Study of Circulation and Mixing Processes in Two-layered Water System: İzmit Bay. In: *Physics of Estuaries and Coastal Seas*, 8th International Biennial Conference, Sponsored by The Netherlands Centre for Coastal Research; The Hague, Netherland (8-12 September). pp. 92-95.
- Balkıs N (2003). The effect of Marmara (İzmit) earthquake on the chemical oceanography of İzmit Bay, Turkey. *Marine Pollution Bulletin* 46:865-878.
- Baştürk O, Tuğrul S, Sunay M, Balkaş T, Morkoç E et al. (1985). Determination of oceanographic characteristics and assimilation capacity of İzmit Bay. NATO TU-WATERS Project, May 1984–May 1985 period. Gebze, Turkey: TÜBİTAK-MAM Publication.
- Beşiktepe ŞT, Sur HI, Özsoy E, Latif MA, Oğuz T et al. (1994). The circulation and hydrography of the Marmara Sea. *Progress in Oceanography* 34(4): 285-333.
- Ergül HA, Aksan S, İpşiroğlu M (2018). Assessment of the consecutive harmful dinoflagellate blooms during 2015 in the İzmit Bay (the Marmara Sea). *Acta Oceanologica Sinica* 37: 91-101. doi: 10.1007/s13131-018-1191-7
- Karakoç FT, Tolun L, Henkelmann B, Klimm C, Okay O et al. (2002). Polycyclic aromatic hydrocarbons (PAHs) and polychlorinated biphenyls (PCBs) distributions in the bay of Marmara Sea: İzmit Bay. *Environmental Pollution* 119: 383-397.
- Morkoç E, Legoviç T, Okay O, Tüfekçi H, Tüfekçi V et al. (2007). Changes of oceanographic characteristics and the state of pollution in the İzmit Bay following the earthquake of 1999. *Environmental Geology* 53: 103-112. doi: 10.1007/s00254-006-0622-5
- Müftüoğlu, AE (2008). Marmara Denizi Haliç ve Körfezleri'nin Hidrodinamik Yapısı. PhD, İstanbul University-IMSM, İstanbul, Turkey (in Turkish with an abstract in English).
- Okay O, Tolun GL, Telli-Karakoç F, Tüfekçi V, Tüfekçi H et al. (2001). İzmit Bay ecosystem after Marmara earthquake and subsequent fire: the long-term data. *Marine Pollution Bulletin* 42:361-369. doi: 10.1016/S0025-326X(00)00163-6
- Sur H (1988). Numerical Modelling Studies of Two-layer Flows in the Dardanelles Strait and the Bay of İzmit. PhD, METU-IMS, Erdemli, İçel, Turkey.
- Turner JS (1973). *Buoyancy Effects in Fluids*. Cambridge, UK: Cambridge University Press.
- Tolun GL, Ergenekon S, Murat Hocaoglu S, Süha Dönertaş A, Çokacar T et al. (2012). Socioeconomic response to water quality: a first experience in science and policy integration for the İzmit Bay coastal system. *Ecology and Society* 17(3): 40. doi: 10.5751/ES-04984-170340
- Tuğrul S, Sunay M, Baştürk Ö, Balkaş TI (1986). The İzmit Bay case study. In: Kullenberg G (editor). *The Role of Oceans as a Waste 498 Disposal Option*. Dordrecht, Holand: Reidel, pp. 243-275.
- Tüfekçi V, Balkıs N, Polat-Beken Ç, Ediger D, Mantıkçı M (2010). Phytoplankton composition and environmental conditions of a mucilage event in the Sea of Marmara. *Turkish Journal of Biology* 34: 199-210.
- Ünlüata Ü, Oğuz T, Latif M, Özsoy E (1990). On the physical oceanography of the Turkish Straits, In: Pratt LJ (editor). *The Physical Oceanography of Sea Straits*. Kluwer Academic Publishers, pp. 25-60.